ELSEVIER

Journal of Chromatography B, 657 (1994) 401–407

JOURNAL OF CHROMATOGRAPHY B: BIOMEDICAL APPLICATIONS

Dependence of electroosmotic flow in capillary electrophoresis on Group I and II metal ions

J.E. Dickens[☆], J. Gorse[*], J.A. Everhart, M. Ryan

Department of Chemistry, Baldwin-Wallace College, Berea, OH 44017, USA

Abstract

The effect of Group I and II metal ions on electroosmotic flow in capillary electrophoresis in fused-silica capillaries is characterized. The electroosmotic mobility of aqueous mobile phases of lithium, sodium, potassium, calcium and barium acetates in fused-silica capillaries is measured as a function of pH at constant voltage. Cross contamination is avoided by using separate columns for each study and pH control is maintained with the aid of He sparging. The shape of a plot of pH *vs.* electroosmotic mobility depends on the particular cation used which in turn depends on the surface sorption properties of the ions. Column history is demonstrated to have an effect on electroosmotic flow and therefore retention times. The resolution of a test mixture is optimal in the lithium-based buffer.

1. Introduction

Capillary electrophoresis (CE) is rapidly becoming a very important separations technique. In terms of speed and efficiency, CE is very competitive with traditional gel electrophoresis and high-performance liquid chromatography (HPLC). One of the main differences between CE and gel electrophoresis, for example, is the use of electroosmotic flow to drive the samples through a capillary.

For many applications electroosmotic flow is advantageous because it produces a very flat flow profile which reduces band broadening of the sample zone in the column and fast elution rates. It has been shown that faster elution rates correspond to higher efficiencies due to a reduction in band broadening caused by axial diffusion of the sample [1]. In some cases reducing or eliminating electroosmotic flow has been shown to be advantageous [*e.g.* 2]. It is important to characterize the parameters which affect electroosmotic flow in order to further improve utility of CE.

Electroosmosis has been shown to be dependent on the viscosity of the buffer solution, the pH, temperature, buffer concentration, capillary tubing material, applied electric field and the addition of organic modifiers such as methanol or acetonitrile [3–8]. The following relationship has been used to describe flow-rate in electroosmosis [9]:

$$V_{eo} = \frac{\epsilon_o \epsilon \zeta}{\eta} E \qquad (1)$$

where V_{eo} is the velocity of the electroosmotic flow, ϵ and ϵ_o are the permittivity of free space and that of the buffer, ζ is the zeta potential, η is

* Corresponding author.

☆ Present address: Department of Chemistry, University of Vermont, Burlington, VT 05405, USA.

0378-4347/94/$07.00
SSDI 0378-4347(94)00074-J

the viscosity and E is the electric field. In Eq. 1 permittivity and viscosity are bulk solution properties and zeta potential is a surface property. These properties are at least somewhat interrelated and they all depend on temperature.

If the bulk solution properties and E are kept constant, then the rate of electroosmotic flow is indicative of changes in the zeta potential. Zeta potential is dependent on factors that change the number of charges at the buffer–glass interface. Among some of the important parameters which affect the charges at interfaces are the differences in the affinity of the two phases for ions on one phase or the other, ionization of surface groups, the physical entrapment of immobile charges and even the sorption of neutral solvent molecules [3,8]. It is known that the surface of silica has silanol groups which are weakly acidic so that zeta potential depends on pH [10]. Plots of pH *vs.* electroosmotic mobility have been characterized as a superposition of a weak acid ionization curve and a sorption isotherm for buffers containing organic solvents [3]. There is no reason to believe that cations all have the same tendency to sorb to a silica surface. One indication of such differences can be seen in studies which involved ion-exchange separations on naked porous silica [11]. Another aspect of the formation of an interface is the rate at which it forms with respect to the conditioning of the surface with buffers which were previously used. We show that the surface "history" is very important in determining the zeta potential and consequently determining electroosmotic flow, since previously sorbed ions and/or solvent molecules may be slow to desorb as the new interface is formed.

2. Experimental

2.1. Apparatus, reagents and materials

The columns were made of fused-silica capillary tubing with an I.D. of 50 μm and 72 cm in length. (Polymicro Technologies, Phoenix, AZ, USA, part No. £2000017). A separate column was prepared for each metal cation of interest so that there was no cross contamination among columns. All columns were made from the same lot of fused-silica capillaries. Each column was conditioned for a half hour with the respective 1.0 M metal hydroxide: LiOH (Matheson Coleman and Bell, Norwood, OH, USA), KOH (J.T. Baker Chemicals Co., Philadelphia, NJ, USA), or NaOH (Fisher Scientific, Fairlawn, NJ, USA). Conditioning solution for Group II ions was made by syphoning the supernatant from saturated solutions of calcium and barium hydroxides. After conditioning, the column was rinsed with HPLC-grade water for a half hour (Milli-Q water system, Millipore, Marlborough, MA, USA) and then rinsed with the running buffer.

The mobile phase buffer solution and the rest of the reagents were reagent-grade or better and prepared with HPLC-grade water; lithium, potassium, calcium and barium acetates (Sigma Scientific, St. Louis, MO, USA), and sodium acetate (Fisher Scientific). After the column was rinsed with HPLC water a 50 mM metal acetate buffer, at the appropriate pH, was eluted through the column. Between each different pH run, the column was rinsed with HPLC-grade water. The specific pH was achieved by adding either the metal hydroxide or acetic acid. The column was then immersed into two mobile phase reservoirs maintained at equal heights to eliminate hydrostatic flow. A relatively large volume of buffer solution (100 ml) was used for the inlet reservoir and was bubbled with helium to maintain a constant pH throughout each run, since the acetates are not particularly good buffers in higher pH ranges. This was considered to be a reasonable trade-off, because we wanted to keep the surface clear of all cations except the metal cation being studied and hydrogen ions. More complicated buffer systems could alter the capillary surface. The pH values reported were an average of the beginning and ending values.

The electric field necessary for the electroosmotic flow was supplied by a regulated high-voltage DC power supply, capable of delivering 0–40 kV (HiPotronics, Brewster, NY, USA). Separations were run at a constant applied voltage of 20 kV. Current across the column was monitored by a multimeter which was interfaced

through the power supply's ammeter and calibrated. The cathode (detector end) and the anode were platinum wire. The column, UV detector, the anode and cathode reservoirs were enclosed in a box with a safety interlock. The enclosed apparatus was maintained at a constant temperature of 30 ± 1°C for all runs with a resistance heater and a thermostatic switch. On-column detection 57 cm from the inlet of column was accomplished with a UV detector fixed at 254 nm (ISCO UA-5 HPLC detector with a custom-made cell to accommodate capillaries). Injections were accomplished via hydrostatic flow by placing the inlet end of the column in a sample vial at a height 10 cm above the inlet level for 12 s. Mesityl oxide at 30 ppm (v/v) in buffer (Aldrich Chemical, Milwaukee, WI, USA) provided a neutral t_o marker for all runs. Each pH data point was repeated a minimum of four times with an R.S.D. of 2% or better.

The column which originally had only sodium acetate in it, was subsequently run with a lithium-based buffer. Initially, this column was re-equilibrated with the sodium acetate buffer and rinsed with HPLC-grade water until a piece of pH paper held at the outlet indicated neutral pH. The electroosmotic flow-rate was determined to be the same as before. Next, the lithium-based buffer was then pumped through until the pH paper showed a change from neutral to alkaline pH. The electric field was then applied at this time and data gathered over a span of 15 h.

The analytes for the test separations were benzoate, phthalate, and 1,5-naphthalenedisulfonate. The running conditions were the same as above, except the pH was maintained at 9.50 for all separations for each column. Separations of analytes were repeated a minimum of three times and were reproducible.

Electroosmotic mobility, μ, was calculated with Eq. 2, where l is the distance from the inlet to the detector window (in cm), L is the distance across the entire column (in cm), V is the voltage and t_o it the elution time for an unretained species (mesityl oxide).

$$\mu = \frac{lL}{Vt_o} \quad (2)$$

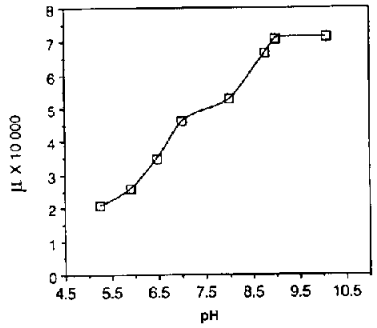

Fig. 1. Lithium acetate at 50 mM, μ *vs.* pH. Mobilities calculated from Eq. 2.

3. Discussion

Figs. 1–3 represent the pH *vs.* μ curves for the lithium, sodium and potassium acetate buffer systems in fused-silica columns respectively. As pH increases, electroosmotic mobility increases

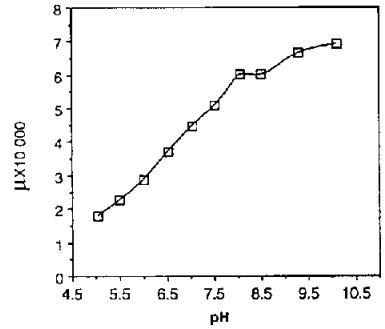

Fig. 2. Sodium acetate at 50 mM, μ *vs.* pH. Mobilities calculated from Eq. 2.

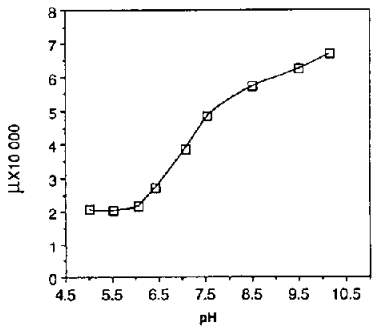

Fig. 3. Potassium acetate at 50 mM, μ *vs.* pH. Mobilities calculated from Eq. 2.

as well. This general trend has been seen before [3,4]. The sigmoidal shape of these curves depends on the ionization of the surface silanols of fused silica. Similarly shaped curves can be seen when the fraction of ionization of a weak acid is plotted *vs.* pH. The inflection point of such curves is at the point where $pH = pK_a$ of the surface. Since silanols behave as weak acids, a plot of charged sites *vs.* pH has a sigmoidal shape similar to an "alpha" plot of the fraction of acid ionized *vs.* pH (see, e.g. [12]). An idealized "alpha" or fractional composition plot for a weak acid with a pK_a of 6.5 is given in Fig. 4. The pK_a value of 6.5 for silica, the approximate value given for the surface silanols on silica surfaces, appears to be appropriate for this work, although there is a fair amount of discrepancy among workers in the field of surface science on this subject [10]. On closer inspection of each of the curves for the individual cations it can be seen that these curves deviate somewhat from the weak acid ionization model. Lithium and sodium even have what appears to be an extra inflection point at the higher pH values which makes their curves resemble titration curves for diprotic acids. Schwer and Kenndler [3] have also noted similar behavior by buffer systems modified with organic solvents. They have suggested that these curves are the result of the superimposition of a titration curve and an adsorption isotherm. This seems reasonable, since there is no a priori reason to assume that the sorption isotherms of lithium, sodium and potassium cations to a silica surface are the same. These ions are all singly charged, but they differ greatly in size as hydrated cations as seen in Table 1 [13]. Although this study does not specifically address the adsorption capacities for these various ions which we employed, they probably follow the same trend that is seen in ion exchange separations on silica. For instance, Smith and Pietrzyk [11] have shown that separations of these cations on naked silica follow the order of elution $Li^+ < Na^+ < K^+$. These curves are very repeatable, including the inflection points. We have been able to generate these pH curves with the same shape between two different researchers several months apart starting with new columns each time and are in agreement within 2–4% of the mobility values. Another factor to consider includes the electrical current across the column. Table 1 shows the current for each system and the mobility of each ion. The ion mobilities increase in the order from $Li^+ < Na^+ < K^+$ and the current (at constant voltage and concentration) increases in the same order. This is because most of the current is carried through the bulk of the buffer solution and the buffer containing ions with the highest mobility carries more current. Higher currents are not desirable because heating causes inefficiency in CE [9]. The lithium buffer is favorable in this regard because it had the lowest current.

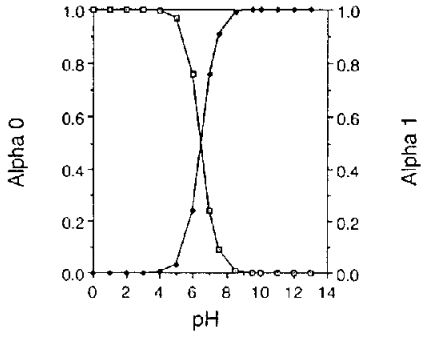

Fig. 4. Fractional concentrations of silanols for $pK_a = 6.5$. Alpha 0 is the fraction of silanols unionized (□) and Alpha 1 is the fraction of ionized silanols (◆).

Table 1
Current at constant voltage

Ion	Ion mobility $(m^2s^{-1}V^{-1}) \times 10^8$	Ion radius (pm)	Current (μA)
Li	4.01	600	23
Na	5.19	450	28
K	7.92	300	48
Ca	6.12	600	49
Ba	6.59	500	55

Table 2 shows the electroosmotic mobilities at three different pH ranges which were taken from the pH *vs.* mobility plots. It is evident that lithium buffer system has the highest rate of electroosmotic flow and potassium has the slowest rate. This finding is in accordance with previous work by Atamna *et al.* [14]. The major

Table 2
Electroosmotic mobility [$\mu(cm^2V^{-1}s^{-1}) \times 10^4$] at different pH values

Buffer	pH 9.30	pH 7.00	pH 5.10
Li	7.10	4.62	2.06
Na	6.65	4.47	1.80
K	6.17	3.87	2.07

For method of calculation see Eq. 2.

difference between our work and ref. 14 is that we used a separate column for each buffer and allowed no cross contamination.

Fig. 5 shows separations of benzoate, phthalate and 1,5-naphthalenedisulfonate acid in the three different alkali metal acetate buffers at pH 9.5. As expected, the lithium-based buffer gave the fastest overall separation. In addition, the lithium-based system exhibited the best resolution. Others have noted an increase in resolution when using a lithium-based buffer [15]. One possible explanation for the greater resolution was the fact that in general, faster elution rates correspond to increased efficiency in CE due to lower band broadening because of less axial diffusion [1].

In order to better understand the dynamics of the buffer/surface equilibration, a lithium-based buffer was introduced into a column previously conditioned with a sodium buffer. Fig. 6 illus-

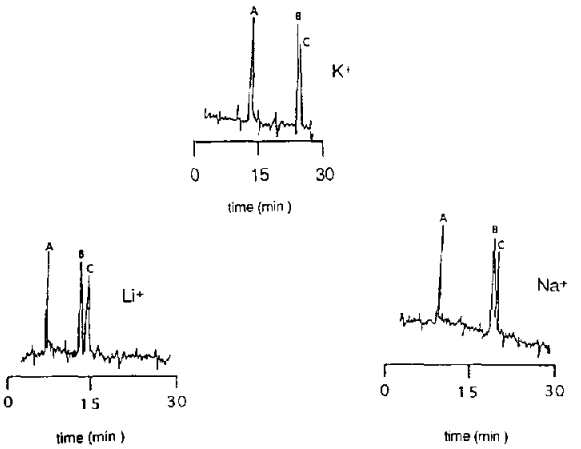

Fig. 5. Separations in the Group I buffer systems. Buffer concentrations were 50 m*M* at pH = 9.5. Peaks: A = benzoate, B = phthalate and C = 1,5-naphthalenedisulfonate.

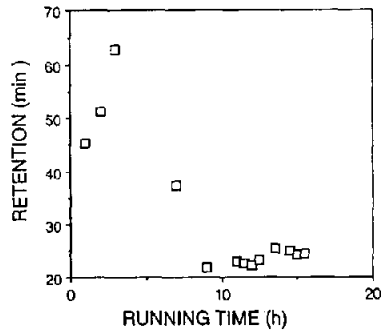

Fig. 6. Retention time of 1,5-naphthalenedisulfonate *vs.* running time. Sodium column with lithium buffer. Running conditions as in Fig. 5.

trates the effect that equilibration time has on retention time. In this figure, it is seen that the system goes through an equilibration time of approximately 10 h. This is an indication of the time it takes to bring about an equilibration of the mobile phase with the surface of the capillary. Further, the equilibrium values of these retention times did not duplicate the values expected from a column in which lithium was used exclusively. It appears as if the sodium surface modification is not completely reversible. This implies that column history is very important in determining electroosmotic flow-rate. If day-to-day retention time precision is important, then columns should be used with only one type of buffer and time should be allotted for them to attain equilibrium with the mobile phase buffer.

At this stage our surface model consists of silanols both ionized and unionized (depending on pH), sorbed ions and solvent molecules. Each surface is in a dynamic equilibrium state and depends on buffer components, the column composition and pH. The zeta potential is indicative of the charge density of the silica buffer interface which in turn depends on the factors cited above is in agreement with others [16–18]. It can take a significant amount of time for equilibrium or a "steady state" to be reached between the buffer and the silica surface.

Calcium and barium acetates represent Group II metal ions and were used to determine their effect on electroosmotic flow. Unfortunately,

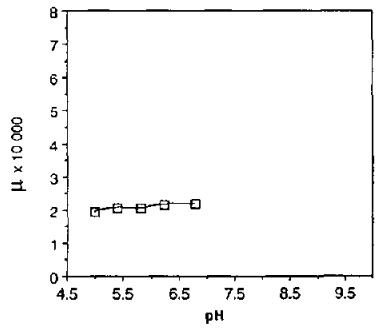

Fig. 7. Calcium acetate at 50 m*M*, μ *vs.* pH. Mobilities calculated from Eq. 2.

these cations form precipitates under alkaline conditions and it was not possible to cover the same pH range as with the Group I metals. Figs. 7 and 8 show the pH *vs.* electroosmotic mobility plots for calcium and barium have a fairly flat response above pH 4.5. The reason for this is possibly that the higher charge of these ions causes them to bind more strongly to the silica surface and it is therefore less influenced by pH changes. An inflection point was determined for the barium system and it was found to be between pH 3.5 and 4.5, in contrast to the inflection points for the Group I systems which were around pH 6–9.5. These buffers appear to hold some promise for use where a low or zero zeta potential is required and they should be potentially more stable to pH shifts in the appropriate range. In Table 1 it can be seen that calcium and barium buffers have high currents which may be a liability in terms of increasing band broadening by thermal effects.

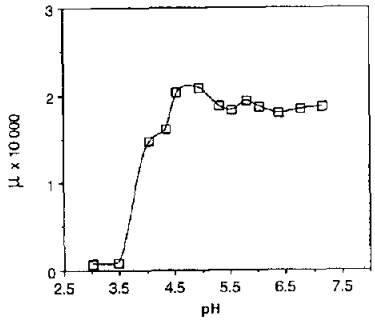

Fig. 8. Barium acetate at 50 m*M*, μ *vs.* pH. Mobilities calculated from Eq. 2.

4. Conclusion

Among the Group I acetates, this study has shown that the lithium buffer gives the highest efficiency of the metal cations studied. This efficiency is attributed to the fastest electroosmotic flow with the lowest current produced by the lithium buffer giving limited amount of column heating. Calcium and barium cations have a more limited pH window, but may be useful because of their flat pH response. It has also been shown that column history is a factor. The optimum conditions for good reproducibility and low equilibration times are maintained if there is no cross contamination of buffer cations in a particular column.

5. Acknowledgements

The authors would like to acknowledge the Research Corporation for the Cottrell College Science Award (No. C-3190) which supported this work and Baldwin-Wallace College for sharing the start-up costs.

6. References

[1] M. Martin, G. Guiochon, Y. Walbroehl and J.W. Jorgenson, *Anal. Chem.*, 57 (1985) 559.
[2] S. Hjerten, *J. Chromatogr.*, 347 (1985) 191.
[3] C. Schwer and E. Kenndler, *Anal. Chem.*, 63 (1991) 1801.
[4] W.J. Lambert and D.J. Middleton, *Anal. Chem.*, 62 (1990) 1585.
[5] J. Gorse, A.T. Balchunas, D.F. Swaile and M.J. Sepaniak, *J. High Resolut. Chromatogr. Chromatogr. Commun.*, 11 (1988) 554.
[6] S. Fujiwara and S. Honda, *Anal. Chem.*, 59 (1987) 487.
[7] K.D. Altria and C.F. Simpson, *Anal. Proc.*, 23 (1986) 453.
[8] M.M. Bushey and J.W. Jorgenson, *J. Microcolumn Sep.*, 1 (1989) 125.
[9] J.H. Knox and I.H. Grant, *Chromatographia*, 24 (1987) 135.
[10] R.K. Iler, *The Chemistry of Silica*, John Wiley and Sons, New York, 1979.
[11] R.L. Smith and D.J. Pietrzyk, *Anal. Chem.*, 56 (1984) 610.

[12] Q. Fernando and M.D. Ryan, *Calculations in Analytical Chemistry*, Harcourt, Brace and Jovanovich, New York, 1982, p. 51.
[13] D. Harris, *Quantitative Chemical Analysis*, W.H. Freeman and Co., New York, 3rd ed., 1991, p. 107.
[14] I.Z. Atamna, C.J. Metral, G.M. Muschik and H.L. Issaq, *J. Liq. Chromatogr.*, 13 (1990) 2517.
[15] A.F. Lecoq, L. Montanarella and S. Di Biase, *J. Microcolumn Sep.*, 5 (1993) 105.
[16] R.J. Hunter, *Zeta Potential in Colloid Science*, Academic Press, London, 1981, Ch. 2.
[17] M.A. Hayes and A.G. Ewing, *Anal. Chem.*, 64 (1992) 512.
[18] K. Salomon, D.S. Burgi and J.C. Helmer, *J. Chromatogr.*, 559 (1991) 69.